The dipole anisotropy of WISE × SuperCOSMOS number counts

C. A. P. Bengaly Jr.,[1,2]⋆ C. P. Novaes[2]† H. S. Xavier[3]‡ M. Bilicki[4,5,6]§ A. Bernui,[2]¶
J. S. Alcaniz,[2]‖

[1]*Department of Physics and Astronomy, University of Western Cape, 7535, Cape Town, South Africa*
[2]*Coordenação de Astronomia e Astrofísica, Observatório Nacional, 20921-400, Rio de Janeiro - RJ, Brazil*
[3]*Instituto de Astrofísica, Geofísica e Ciências Atmosféricas, Universidade de São Paulo, 05508-090, São Paulo - SP, Brazil*
[4]*Leiden Observatory, Leiden University, 2333, P.O. Box 9513, NL-2300 RA Leiden, The Netherlands*
[5]*National Center for Nuclear Research, Astrophysics Division, P.O. Box 447, 90-950, Łódź, Poland*
[6]*Janusz Gil Institute of Astronomy, University of Zielona Góra, ul. Szafrana 2, 65-516 Zielona Góra, Poland*

15 May 2022

ABSTRACT

We probe the validity of the isotropy hypothesis of the Universe, one of the foundations of modern Cosmology, with the WISE × SuperCOSMOS data set. This is performed by searching for dipole anisotropy of galaxy number counts in different redshift shells in the $0.10 < z \leq 0.35$ range. We find that the dipole direction is in concordance with most of previous analyses in the literature, however, its amplitude is only consistent with ΛCDM-based mocks when we adopt the cleanest sample of this catalogue, except for the $z < 0.15$ data, which exhibits a persistently large dipole signal. Hence, we obtain no significant evidence against the large-scale isotropy assumption once the data are purified from stellar contamination, yet our results in the lowest redshift range are still inconclusive.

Key words: Cosmology: observations; Cosmology: theory; (cosmology:) large-scale structure of the Universe;

1 INTRODUCTION

The current standard model of cosmology, called ΛCDM, assumes Friedman-Lemaître-Robertson-Walker its background metric, and that the Universe is approximately homogeneous and isotropic on large scales, a feature of the so-called 'Cosmological Principle' (CP). Despite the good agreement between ΛCDM and a plethora of cosmological observations (e.g. Ade et al. 2016; Alam et al. 2016), direct tests of the CP need to be performed in order to assess whether it is a valid cosmological assumption or just mathematical simplification. Persistent lack of isotropy or homogeneity on large scales would require a complete reformulation of the current cosmological scenario, and thus of our understanding of the Universe.

It is well accepted that the spatial distribution of cosmic objects becomes statistically homogeneous on scales around $100 - 150$ Mpc/h (Hogg et al. 2005; Scrimgeour et al. 2012; Pandey & Sarkar 2016; Laurent et al. 2016; Ntelis et al. 2017), and that the CMB temperature dipole is the only major non-primordial anisotropy we observe in the Universe, since it is interpreted as our peculiar motion relative to CMB instead of an actual cosmological signal (Kogut et al. 1993; Aghanim et al. 2014)[1]. However, this dipole has yet to be identified in the large-scale structure (LSS) with sufficient significance. Some estimates of the dipole in projected distributions of galaxies were carried out, but no evidence for signals larger than allowed by the standard cosmological model (within 3σ confidence level) was found using optical or infrared catalogues (Itoh et al. 2010; Gibelyou & Huterer 2012; Appleby & Shafieloo 2014; Yoon et al. 2014; Alonso et al. 2015; Bengaly et al. 2017), although similar analyses in the radio frequency presented more ambiguous results (Blake & Wall 2002; Rubart & Schwarz 2013; Tiwari & Nusser 2016; Colin et al. 2017).

In light of these results, we probe the isotropy of the large-scale structure using the recently published WISE × SuperCOSMOS (hereafter WI×SC) catalogue (Bilicki et al. 2016)[2] by looking for a dipole term in its projected distribution of galaxies in a similar framework as in Gibelyou & Huterer (2012). We also check for concordance between the observational data and their respective mocks assuming the ΛCDM matter power spectrum as a fiducial model, similarly to previous analyses (Gibelyou & Huterer 2012; Alonso et al. 2015; Bengaly et al. 2017). As the WI×SC sample contains photometric redshift (photo-*z*) information for its galax-

⋆ E-mail: carlosap87@gmail.com
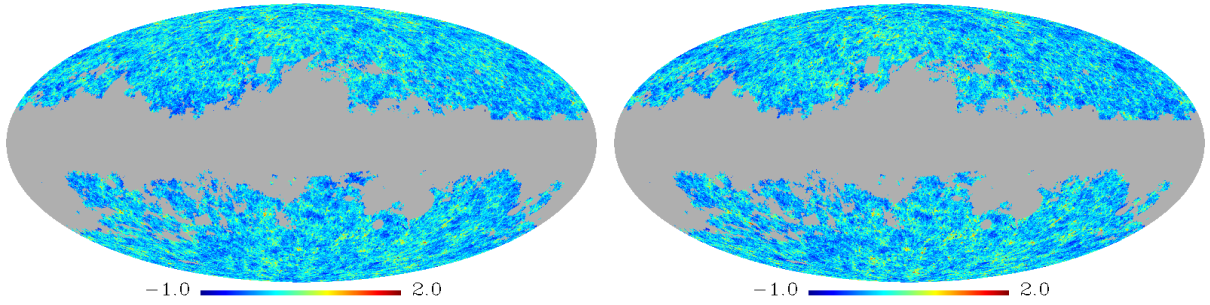† E-mail: camilanovaes@on.br
‡ E-mail: hsxavier@if.usp.br
§ Email: bilicki@strw.leidenuniv.nl
¶ E-mail: bernui@on.br
‖ E-mail: alcaniz@on.br

---

[1] We will refer to it as the kinematic dipole hereafter.
[2] http://ssa.roe.ac.uk/WISExSCOS

Figure 1. *Left panel:* The density contrast of galaxy number counts (clipped at 2.0 to ease visualisation) of the WI×SC Fiducial sample in the $0.10 < z \leq 0.35$ range, i.e., the full sample analysed here. *Right panel:* Same as the left panel, but for the SVM sample. The grey area corresponds to the masked region as discussed in section 2.
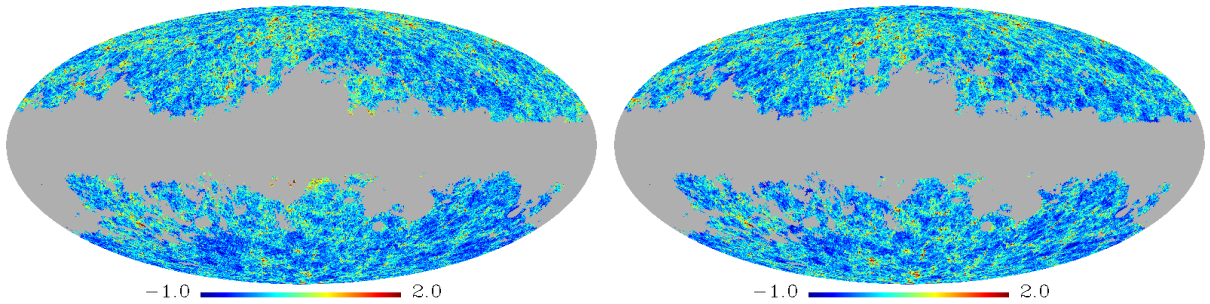

Figure 2. Same as Fig. 1, but for galaxies within $0.10 < z \leq 0.15$ only.

ies, we can perform a tomographic analysis of the number count dipole at $z > 0.10$ for the first time, thus allowing us to probe how the dipole evolves when reaching deeper scales and, furthermore, whether it agrees with their expected amplitudes in the ΛCDM paradigm in each redshift shell. Strong discrepancies between the real data and these simulations would hint at potential evidence against the cosmic isotropy assumption, unless we are restricted by persisting systematics. We therefore extend the analysis of Bengaly et al. (2017) where another WISE-based catalogue was used, namely WISE-2MASS (W2M, Kovács & Szapudi 2015), which not only was shallower than WI×SC but also did not include redshift information, even of photometric nature, and it comprised 10 times fewer sources.

2 DATA SELECTION

The WI×SC photo-z catalogue (Bilicki et al. 2016) is based on a cross-match of two all-sky samples, WISE (Wright et al. 2010) and SuperCOSMOS (Peacock et al. 2016). This dataset is flux-limited to $B < 21$, $R < 19.5$ (both AB), and $13.8 < W1 < 17$ ($3.4\,\mu m$, Vega) and provides photo-zs for all the included sources, ranging from $0 < z < 0.4$ (mean $\langle z \rangle \simeq 0.2$) with typical scatter $\sigma_z/(1+z) = 0.033$ (15% median photo-z error). The data come with a fiducial mask which removes low Galactic latitudes ($|b| \leq 10°$ up to $|b| \leq 17°$ by the Bulge), areas of high Galactic extinction ($E(B-V) > 0.25$), as well as other contaminated regions. Here we however apply more strict cuts to avoid selection effects due to extinction, namely $E(B-V) > 0.10$, and require $0.10 < z_{phot} < 0.35$ to remove low-redshift
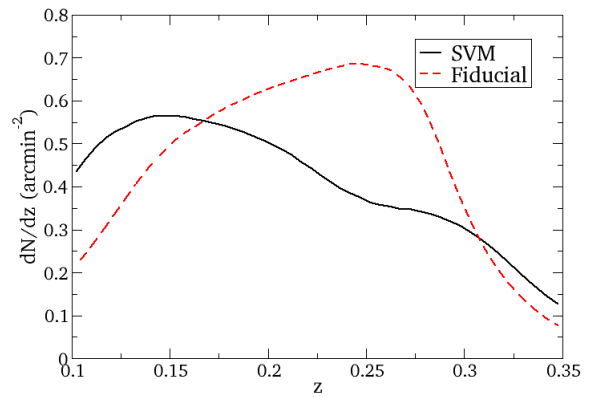
Figure 3. The redshift distribution for the Fiducial sample (red dashed curve) and the SVM one (black solid curve), both given in counts per square arcminute per redshift bin.

prominent structures as well as the high-redshift tail of WI×SC, where the data is very sparse.

The basic WI×SC dataset by Bilicki et al. (2016) was additionally purified from stellar (blends) and quasar contamination via specific colour cuts, which were dependent on the distance from the Bulge in the case of star removal. This gave a sample with

a relatively uniform surface density over the sky, although some patterns of residual stellar contamination were still present. As purity is more important for our purposes than completeness, we thus applied an additional colour cut of $W1 - W2 > 0.2$, which should guarantee very efficient star removal (Jarrett et al. 2017). We will call this WI×SC sample with the additional cleanup 'Fiducial' from now on. In an alternative approach to galaxy identification in WI×SC, Krakowski et al. (2016) used the Support Vector Machines (hereafter SVM) classification algorithm and obtained a purer galaxy sample than the main WI×SC one but less complete. The SVM dataset comes with probability estimates of sources belonging to a given class, and we applied a conservative cut of $p_{gal} > 2/3$, so that our selected objects have at least twice the probability of being a galaxy rather than any other class.

After applying the WI×SC mask as well as our additional cuts on $E(B - V)$ and photo-z, we obtained samples of 9.5 and 8.3 million galaxies for the Fiducial and SVM datasets, respectively, over $f_{sky} \simeq 0.545$, of median redshifts $z_{med} \simeq 0.22$ (Fiducial) and $z_{med} \simeq 0.20$ (SVM), as shown in Figure 3. Number count density maps of these samples for the full redshift range ($0.10 < z \leq 0.35$) are featured in Fig. 1, whereas Fig. 2 displays only the galaxies within the $0.10 < z \leq 0.15$ range. All maps were plotted using HEALPix (Górski et al. 2005) resolution of $N_{side} = 128$ (pixel size of $\sim 0.5°$).

3 METHODOLOGY

The isotropy of galaxy number counts is estimated with the delta-map method developed in Bengaly et al. (2017) (see also Alonso et al. 2015), in which the sky is decomposed into 768 large HEALPix cells ($N_{side} = 8$), and hemispheres are constructed using the respective pixel centres as symmetry axes. The delta-map is then computed as

$$\Delta_i = 2 \times \left(\frac{n_i^U - n_i^D}{n_i^U + n_i^D} \right), \qquad (1)$$

where $n_i^j \equiv N_i^j/(4\pi f_{sky,i}^j)$ are counts in the i-th hemisphere, $i \in 1, ..., 768$, j represents the hemispheres indexes "up" (U) and "down" (D) defined according to this pixellisation scheme, whereas N_i^j and $f_{sky,i}^j$ are the total number of objects and the observed fraction of the sky encompassed in each of these hemispheres, respectively.

The dipole of the galaxy number counts is obtained from expression 1 by expanding the delta-map into spherical harmonics and then setting all $\{a_{\ell m}\}$'s to zero except for the a_{1m} cases, from which we obtain $\Delta_{dip} = \sum a_{1m} Y_{1m}$. Therefore, we quote the maximum value of this quantity as our dipole amplitude A, in addition to the direction where it points to. In this work, the WI×SC catalogue is additionally decomposed into redshift shells before the delta-map calculation: cumulative ones i.e. $0.10 < z \leq 0.15; 0.10 < z \leq 0.20; ...; 0.10 < z \leq 0.35$, and disjoint ones: $0.10 < z \leq 0.15; 0.15 < z \leq 0.20; ...$; etc. As we have $\sim 10^6$ galaxies in each of these shells, the Poisson Noise contribution to the dipole is sub-dominant with respect to its total signal, being thus quoted as its uncertainty.

The statistical significance of the delta-map dipoles is calculated from WI×SC mock catalogues produced with the FLASK code[3] (Xavier et al. 2016). These mocks are full-sky lognormal realisations of the density field in redshift shells based on the input

angular power spectra $C_\ell^{(z_i z_j)}$ (z_i and z_j denoting different redshift shells) provided by CAMB SOURCES (Challinor & Lewis 2011), which are Poisson-sampled according to the WI×SC selection function. The input $C_\ell^{(z_i z_j)}$ were computed for redshift distributions that are convolutions of the $\delta z = 0.05$ shells with Gaussian distributions with $\sigma_z/(1 + z) = 0.033$ (representing WI×SC photo-z errors) using ΛCDM best-fit parameters (Ade et al. 2016), and they include linear redshift space distortions, gravitational lensing distortions of the volume elements and non-linear contributions modelled by HALOFIT (Smith et al. 2003; Takahashi et al. 2012). We applied a linear scaling factor to each $C_\ell^{(z_i z_j)}$ – playing a role similar to galaxy bias – which was used to match the variances of counts in pixels to the ones observed in the real data.

We additionally compared the Fiducial dataset source distribution to SDSS (York et al. 2000) in a 1°-wide strip centred on declination $\delta = 30°$ and estimated that it still contained a fraction f_{star} of stars that is well fitted by $f_{star} = 0.71 \exp(-0.09|b|) + 0.013$. Therefore, we Poisson sampled stars according to this distribution and included them in our mocks. By adjusting the selection function normalisation and the $C_\ell^{(z_i z_j)}$ scaling factors, we made our simulations match the Fiducial dataset in terms of f_{star}, mean number of objects (galaxies + stars) and variance in the pixels[4].

Following this prescription, we produced 1000 full-sky mocks of both Fiducial and SVM datasets in each $\delta z = 0.05$ photo-z bin, spanning the $0.10 < z \leq 0.35$ range, using the same resolution of the real data maps ($N_{side} = 128$). From these realisations, we computed the fraction of realisations featuring a dipole amplitude at least as large as the real data for each z-bin analysed, hereafter quoted as p-values, once the mask described before is properly taken into account.

4 RESULTS

The dipoles resulting from the delta-map analyses of the two WI×SC samples are shown for the full redshift range in Fig. 4, while the dipole directions and amplitudes for each redshift bin are presented in Table 1 for both Fiducial and SVM datasets. We readily verify the dipole amplitude decreases when probing the number counts on deeper scales, as it goes from $A \simeq 0.10$ in the thinnest ($0.10 < z \leq 0.15$) to $A \simeq 0.03$ in the thickest ($0.10 < z \leq 0.35$) cumulative shell, thus confirming the discussion and results of Gibelyou & Huterer (2012).

We also stress that the directions of the number count dipoles in cumulative redshift shells, specially the redshift range $0.10 < z \leq 0.35$ of the SVM dataset, are in good agreement with similar analyses in the literature. For instance, Bengaly et al. (2017) obtained a dipole anisotropy of $(l, b) = (323°, -5°)$ with $A = 0.0507$ in the W2M catalogue, which peaks at $z \sim 0.14$, whereas Yoon et al. (2014) and Alonso et al. (2015) found, using different methods, the directions $(l, b) = (310°, -15°)$ and $(320°, 6°)$ with $A = 0.051$ and $A = 0.028$ from the W2M and 2MASS photo-z (2MPZ, Bilicki et al. (2014), with $\langle z \rangle \simeq 0.08$) datasets, respectively. On the other hand, the Fiducial sample dipole is more consistent with the direction found in Appleby & Shafieloo (2014), i.e., $(l, b) = (315°, 30°)$, whose authors adopted the 2MPZ sample as well. A quantitative assessment of the concordance between these dipole directions is featured in Tab. 2, where can calculate the probabilities P_θ that the

---
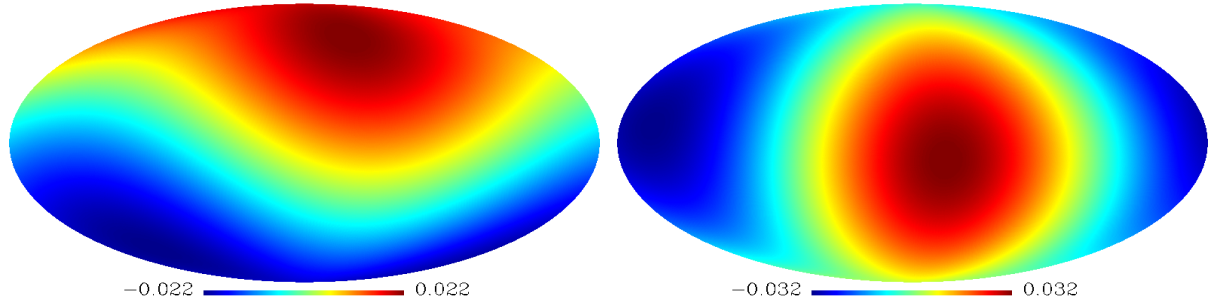
Figure 4. *Left panel:* The Delta-map dipole of the WI×SC Fiducial data set in the $0.10 < z \leq 0.35$ range. *Right panel:* Same as the left panel, but for the WI×SC SVM galaxies. Both maps are represented in galactic coordinates.

redshift bin (Fiducial)	$A\ (10^{-1})$	(l, b)	p-value
$0.10 < z \leq 0.15$	1.474 ± 0.013	$(57°, 70°)$	< 0.001
$0.10 < z \leq 0.20$	0.701 ± 0.008	$(21°, 70°)$	< 0.001
$0.10 < z \leq 0.25$	0.394 ± 0.006	$(346°, 70°)$	0.001
$0.10 < z \leq 0.30$	0.250 ± 0.006	$(318°, 61°)$	0.084
$0.10 < z \leq 0.35$	0.225 ± 0.005	$(320°, 60°)$	0.129
$0.15 < z \leq 0.20$	0.303 ± 0.011	$(325°, 44°)$	0.129
$0.20 < z \leq 0.25$	0.200 ± 0.010	$(273°, -10°)$	0.332
$0.25 < z \leq 0.30$	0.293 ± 0.011	$(263°, -42°)$	0.017
$0.30 < z \leq 0.35$	0.112 ± 0.020	$(28°, -59°)$	0.773
redshift bin (SVM)	$A\ (10^{-1})$	(l, b)	p-value
$0.10 < z \leq 0.15$	0.863 ± 0.011	$(29°, 66°)$	< 0.001
$0.10 < z \leq 0.20$	0.417 ± 0.008	$(342°, 27°)$	0.019
$0.10 < z \leq 0.25$	0.371 ± 0.007	$(333°, -3°)$	0.010
$0.10 < z \leq 0.30$	0.320 ± 0.006	$(335°, -7°)$	0.010
$0.10 < z \leq 0.35$	0.316 ± 0.006	$(340°, -9°)$	0.007
$0.15 < z \leq 0.20$	0.674 ± 0.011	$(315°, -34°)$	< 0.001
$0.20 < z \leq 0.25$	0.682 ± 0.012	$(311°, -52°)$	< 0.001
$0.25 < z \leq 0.30$	0.166 ± 0.014	$(13°, -49°)$	0.236
$0.30 < z \leq 0.35$	0.370 ± 0.018	$(19°, -19°)$	< 0.001

Table 1. The amplitude, direction, statistical significance (given in p-values) of the WI×SC dipole (cols. 2, 3, 4, respectively) obtained from the Fiducial (top) and SVM (bottom) samples. The uncertainties of A are given by the Poisson noise contribution to its signal, while the error bars of its direction correspond to the pixel size of $7.33°$.

alignments between the corresponding directions would occur at random, given by the ratio of the area covered by angular separations smaller than the one observed to the total area:

$$P_\theta = \frac{1}{4\pi} \int_0^\theta 2\pi \sin\theta' \mathrm{d}\theta' = \frac{1 - \cos\theta}{2}, \qquad (2)$$

given $\cos\theta = \sin b_1 \sin b_2 + \cos b_1 \cos b_2 \cos(l_1 - l_2)$. From that table, we note that all these directions are moderately distant from the CMB dipole, located at $(l, b) = (246°, 48°)$ in the heliocentric rest frame, with the Fiducial dataset the closest one (at $43°$ apart, they fit together in a $f_{sky} = 0.15$ patch of the sky), which is probably due to the limited depth, sky coverage and size of these datasets (see Yoon & Huterer (2015) for the galaxy survey specifications required to probe the kinematical dipole with $> 3\sigma$ confidence level). Still, the agreement between different methods and observational data indicates that the anisotropy directions found in these analyses are indeed robust.

The comparison between the dipole amplitude of the actual observations and lognormal WI×SC mocks show only marginal

agreement for the SVM dataset, yet the Fiducial one performs considerably better in this sense. We find that both SVM and Fiducial data show a larger dipole amplitude than the mocks in the shallowest redshift shell, that is, $0.10 < z \leq 0.15$, but the agreement improves when the cumulative redshift shells encompass more distant galaxies. This can be noted even more clearly for the Fiducial sample, where $p-$value > 0.05 in the two thickest redshift shells. For the SVM dataset, however, less than $\sim 2\%$ of the realisations have larger A than the real data in these same shells. In the tomographic z-bins, we found good agreement between the Fiducial sample and its mocks in most of these bins, except for $0.25 < z \leq 0.30$ which, interestingly, is the redshift shell in which the SVM dipole amplitude agrees the most with these simulations.

From these results, we conclude that the Fiducial dataset shows much better concordance with its respective ΛCDM-based mocks than the SVM one, which we ascribe to the colour cut which cleaned the former sample of stars as described in Sec. 2, while the latter still has stellar contamination showing especially at the lowest redshifts. Therefore, we obtain no statistically significant evidence against the large-scale isotropy assumption once we account for the dataset purification in $z > 0.15$. However, the results are still inconclusive for the shallowest redshift ranges, where both datasets show excellently aligned dipoles with amplitudes larger than those of simulations.

5 CONCLUSIONS

In this work, we examined the isotropy of the large-scale structure through the directional dependence of galaxy number counts in the WISE × SuperCOSMOS catalogue. To do so, we adopted a hemispherical comparison method whose dipole contribution provided our diagnostic of cosmological anisotropy. The observational samples consisted of two datasets, namely 'Fiducial' and 'SVM', which differ in how galaxies were identified in them: through colour cuts in the former, and by means of automatised classification in the latter. Thanks to the availability of redshift information, we were able to perform this test in tomographic z-bins, which gave a natural extension of the analysis carried out in Bengaly et al. (2017) with the WISE-2MASS sample. We found marginal agreement or better between the dipole directions we obtained and those from previous analyses in the literature. In addition, we obtained that only the Fiducial sample presented a dipole amplitude consistent with mock realisations when $z > 0.15$. Below this redshift range, all datasets exhibit a larger dipole than predicted by the simulations.

Albeit we still cannot probe the kinematical dipole with this dataset catalogue because of its limited specifications (Yoon &

Dipole	CMB	BengalyFid	BengalySVM	BengalyW2M	Alonso15	Yoon14	Appleby14	LowzFid	LowzSVM
CMB	-	0.132	0.581	0.457	0.369	0.455	0.21	0.264	0.269
BengalyFid	0.132	-	0.336	0.289	0.206	0.374	0.068	0.104	0.068
BengalySVM	0.581	0.336	-	0.023	0.047	0.067	0.151	0.536	0.44
BengalyW2M	0.457	0.289	0.023	-	0.01	0.02	0.095	0.553	0.457
Alonso15	0.369	0.206	0.047	0.01	-	0.041	0.045	0.472	0.38
Yoon14	0.455	0.374	0.067	0.02	0.041	-	0.148	0.67	0.581
Appleby14	0.21	0.068	0.151	0.095	0.045	0.148	-	0.296	0.223
LowzFid	0.264	0.104	0.536	0.553	0.472	0.67	0.296	-	0.009
LowzSVM	0.269	0.068	0.44	0.457	0.38	0.581	0.223	0.009	-

Table 2. The probability that randomly picked directions are closer than the distance between the corresponding dipoles, in which 'BengalyFid' and 'BengalySVM' corresponds to the full Fiducial and SVM samples analysed here, respectively, while both 'Lowz' cases consists of their $0.10 < z \leq 0.15$ results. The remaining directions were obtained in Aghanim et al. (2014); Yoon et al. (2014); Appleby & Shafieloo (2014); Alonso et al. (2015); Bengaly et al. (2017), respectively.

Huterer 2015), we were able to show that the dipole amplitude indeed decreases on deeper scales, and that there is consistency between the SVM dipole direction with similar datasets. However, the Fiducial one shows much better agreement with simulations than the SVM, which we credit to a more rigorous criterion to eliminate stars from the original catalogue. Still, this procedure cannot explain the large A values obtained in the $0.10 < z \leq 0.15$ redshift shell, a result whose origin is unclear. According to Rubart et al. (2014), the presence of local LSS underdensities can increase the dipole anisotropy in the number counts, being thus a possible explanation for this signal. A more thorough investigation of this hypothesis will be pursued in the future.

This work presents the first contribution of the WI×SC catalogue to Cosmology in the form of an updated test of the large-scale isotropy of the Universe, in which we found no significant departure from this fundamental hypothesis, yet we are still very limited by the completeness and systematics of the available data. Nonetheless, the WI×SC data set can be considered a testbed for forthcoming surveys, especially LSST (Abell et al. 2009) and SKA (Schwarz et al. 2015), as they will reach much deeper scales on large sky areas and, therefore, will enable much more precise tests of the CP in the years to come (Itoh et al. 2010; Schwarz et al. 2015; Yoon & Huterer 2015).

REFERENCES

Abell, P. A. et al. [LSST Red Book 2.0], 2009, arXiv:0912.0201
Ade, P. A. R. et al. [Planck Collaboration], 2016, Astron. Astrop. 594, A13
Aghanim, N. *et al.* [Planck Collaboration], 2014, Astron. Astrophys. 571, A27
Alam, S. *et al.* [SDSS Collaboration], 2016, arXiv:1607.03155
Alonso, D. *et al.*, 2015, Mon. Not. Royal Ast. Soc., 449, 670
Appleby. S. & Shafieloo, A., 2014, JCAP, 10, 070
Bengaly, C. A. P. *et al.*, 2017, Mon. Not. Roy. Astr. Soc. 464, 1, 768
Bilicki, M. *et al.*, 2014, Astrophys. J. Suppl. Ser. 210, 1, 9
Bilicki, M. *et al.*, 2016, Astrophys. J. Suppl. Ser., 225, 5
Blake, C. & Wall, J. V., 2002, Nature, 416, 150
Challinor, C. & Lewis, C., 2011, Phys. Rev. D 84, 43516
Clarkson, C. & Maartens, R., 2010, Class. Quant. Grav., 27, 124008
Colin, J. *et al.*, 2017, arXiv:1703.09376
Gibelyou, C. & Huterer, D., 2012, Mon. Not. Roy. Astr. Soc. 427, 1994
Górski, K. M. *et al.*, 2005, Astrophys. J. 622, 759
Hogg, D. W. *et al.*, 2005, Astrophys. J. 624, 54
Itoh, Y., Yahata, K. & Takada, M., 2010, Phys. Rev. D 82, 4, 043530
Jarrett, T. H. *et al.*, 2017, Astrophys. J., 836, 2, 182
Kogut, A. *et al.*, 1993, Astrophys. J. 419, 1
Kovács, A. & Szapudi, I., 2015, Mon. Not. Roy. Astr. Soc. 448, 2, 1305
Krakowski, T. *et al.*, 2016, Astron. Astrophys. 596, A39
Laurent, P. *et al.*, 2016, JCAP 2016, 11, 060
Ntelis, P. *et al.* 2017, JCAP 2017, 06, 019
Pandey, B. & Sarkar, S., 2016, Mon. Not. Roy. Astr. Soc. 460, 2, 1519
Peacock, J. A. *et al.*, 2016, Mon. Not. Roy. Astr. Soc. 462, 2, 2085
Rubart, M. & Schwarz, D. J., 2013, Astron. Astrophys. 555, A117
Rubart, M., Bacon, D. & Schwarz, D. J., 2014, Astron. Astrophys. 565, A111
Schwarz, D. J. *et al.*, 2015, PoS AASKA14, 032
Scrimgeour, M. *et al.*, 2012, Mon. Not. Roy. Astr. Soc. 425, 116
Smith, R. E. *et al.*, 2003, Mon. Not. Roy. Astr. Soc. 341, 1311
Takahashi R. *et al.*, 2012, Astrophys. J., 761, 152
Tiwari, P. & Nusser, A., 2016, JCAP 2016, 03, 062
Wright, E. L. *et al.*, 2010, The Astron. J. 140, 6, 1868
Xavier, H. S., Abdalla, F. B. & Joachimi, B. 2016, Mon. Not. Roy. Astr. Soc. 459, 4, 3693
Yoon, M. *et al.*, 2014, Mon. Not. Roy. Astr. Soc. 445, L60
Yoon, M. & Huterer, D., 2015, Astrophys. J. 813, 1, L18
York, D. G. *et al.*, 2000, The Astron. J. 120, 1579

This paper has been typeset from a TEX/LATEX file prepared by the author.